Article

Enzyme-like Specificity in Zeolites: A Unique Site Position in Mordenite for Selective Carbonylation of Methanol and Dimethyl Ether with CO

Mercedes Boronat, Cristina Marti#nez-Sa#nchez, David Law, and Avelino Corma

J. Am. Chem. Soc., **2008**, 130 (48), 16316-16323 • DOI: 10.1021/ja805607m • Publication Date (Web): 06 November 2008

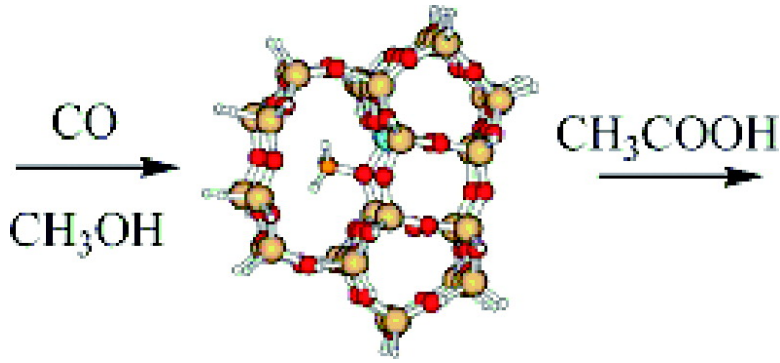

More About This Article

Additional resources and features associated with this article are available within the HTML version:

- Supporting Information
- Access to high resolution figures
- Links to articles and content related to this article
- Copyright permission to reproduce figures and/or text from this article

View the Full Text HTML

J|A|C|S
ARTICLES

Published on Web 11/06/2008

Enzyme-like Specificity in Zeolites: A Unique Site Position in Mordenite for Selective Carbonylation of Methanol and Dimethyl Ether with CO

Mercedes Boronat,† Cristina Martínez-Sánchez,† David Law,‡ and Avelino Corma*,†

Instituto de Tecnología Química, Universidad Politécnica de Valencia-CSIC, Av. de los Naranjos s/n, 46022 Valencia, Spain, and BP Chemicals, Hull Research & Technology Centre, Saltend, Hull HU12 8DS, U.K.

Received July 18, 2008; E-mail: acorma@itq.upv.es

Abstract: The mechanism of methanol carbonylation at different positions of zeolite MOR is investigated by quantum-chemical methods in order to discover which are the active sites that can selectively catalyze the desired reaction. It is shown that when methanol carbonylation competes with hydrocarbon formation, the first reaction occurs preferentially within 8MR channels. However, the unique selectivity for the carbonylation of methanol and dimethyl ether in mordenite is not only due to the size of the 8MR channel: neither process occurs equally at the two T3-O31 and T3-O33 positions. We show that only the T3-O33 positions are selective and that this selectivity is due to the unusual orientation of the methoxy group in relation to the 8MR channel (parallel to the cylinder axis). Only in this situation does the transition state for the attack of CO fit perfectly in the 8MR channel, while the reaction with methanol or DME is sterically impeded. This result explains why T3-O31, while also located in the 8MR channel of mordenite, is not as selective as the T3-O33 position and why ferrierite, although it contains 8MR channels, is less selective than mordenite. The competing effect of water is explained at the molecular level, and the molecular microkinetic reaction model has been established.

1. Introduction

Sustainability in chemistry will be improved by finding selective catalysts that can minimize the use of raw materials and the formation of subproducts. One way to achieve this is to go through the molecular design of well-structured solid catalysts having pore dimensions and topologies that can stabilize the transition state for the desired reaction. If this idea is followed with the focus of attention on zeolites, cases may be found in where it is not enough to locate the active sites in a particular channel: in order to achieve unique selectivities, it may be necessary to perform the reaction at a specific position among all of the possible ones existing in the given channel. This is the case for the selective carbonylation of methanol and dimethyl ether (DME) by CO. This is an important industrial reaction, since acetic acid is manufactured industrially by carbonylation of methanol with CO using Rh or Ir organometallic complexes as catalysts and iodide compounds as promoters.[1,2] Thus, from an environmental point of view, it would be of much interest to find a selective solid that catalyzes the reaction in the absence of iodide compounds. Acid zeolites are able to catalyze the carbonylation of alcohols at low temperatures and atmospheric pressure without requiring the use of a halide cocatalyst.[3−6] The mechanism of alcohol carbonylation catalyzed by acid zeolites involves adsorption and reaction of the alcohol on a Brønsted acid site to form the methoxy species, which reacts with CO to form an acylium cation that in turn reacts with H_2O to give the corresponding acid[7,8] (Scheme 1).

Scheme 1. Mechanism of Alcohol Carbonylation Catalyzed by Acid Zeolites

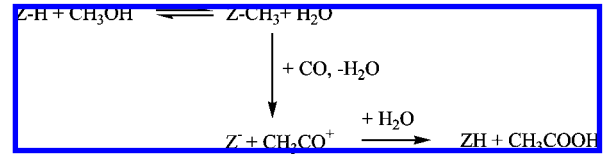

It has recently been reported that the zeolite-catalyzed carbonylation of DME with CO in the absence of H_2O shows an excellent selectivity to give methyl acetate at low temperatures (423−463 K), and a mechanism in which the rate-limiting step is the attack on a surface methoxide group by CO has been proposed on the basis of kinetic experiments and NMR

† Universidad Politécnica de Valencia-CSIC.
‡ BP Chemicals.

(1) Paulik, F. E.; Roth, J. F. *Chem. Commun.* **1968**, 1578.
(2) Sunley, G. J.; Watson, D. J. *Catal. Today* **2000**, *58*, 293.
(3) Fujimoto, K.; Shikada, T.; Omata, K.; Tominaga, H. *Chem. Lett.* **1984**, 2047.
(4) Stepanov, A. G.; Luzgin, M. V.; Romannikov, V. N.; Zamaraev, K. I. *J. Am. Chem. Soc.* **1995**, *117*, 3615.
(5) Ellis, B.; Howard, M. J.; Joyner, R. W.; Reddy, K. N.; Padley, M. B.; Smith, W. J. *Stud. Surf. Sci. Catal.* **1996**, 771.
(6) Smith, W. J. Patent EP0596632A1 to BP Chemicals Limited, 1993.
(7) Xu, Q.; Inoue, S.; Tsumori, N.; Mori, H.; Kameda, M.; Tanaka, M.; Fujiwara, M.; Souma, Y. *J. Mol. Catal.* **2001**, *170*, 147.
(8) (a) Stepanov, A. G.; Luzgin, M. V.; Romannikov, V. N.; Sidelnikov, V. N.; Zamaraev, K. I. *J. Catal.* **1996**, *164*, 411. (b) Luzgin, M. V.; Romannikov, V. N.; Stepanov, A. G.; Zamaraev, K. I. *J. Am. Chem. Soc.* **1996**, *118*, 10890.

10.1021/ja805607m CCC: $40.75

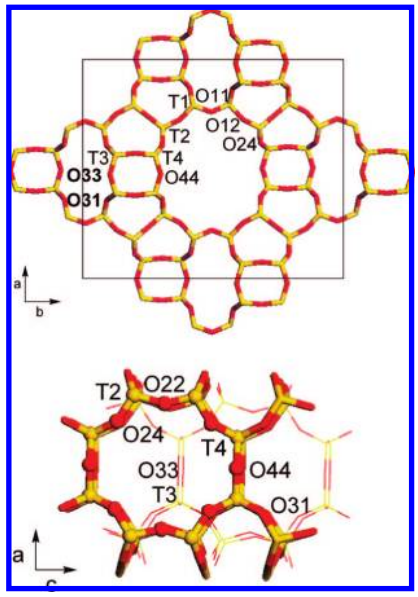

Figure 1. Structure of MOR in the (top) *c* and (bottom) *b* directions. The atom-labeling scheme is also shown.

spectroscopy.[9−12] When methanol is used instead of DME, conversion is lower and higher reaction temperatures are required, with the corresponding formation of hydrocarbons that diminishes the selectivity for giving the desired carbonylation product and produces catalyst deactivation.[5,6,13] Among the different zeolite structures that have been tested as catalysts for the carbonylation of methanol, mordenite is by far the most active and selective, followed by ferrierite. Since the common feature of these two zeolites is the presence of eight-membered rings (8MRs), it has been suggested that the reaction of methoxy groups with CO occurs selectively within these 8MR channels,[12] while the acid sites present in the 12MR channels would be responsible for the formation of hydrocarbons when working at higher temperatures. The essential role that zeolite structure, pore size, and confinement effects play in the activation of alkanes has been discussed in the literature,[14,15] and the special features of acid sites in MOR side pockets and their relation to the better catalytic performance of this particular zeolite for a number of reactions have been emphasized.[16−18]

Because of the fundamental and potential industrial interest of the carbonylation of methanol and DME with mordenite, it is of much interest to discover which are the active sites involved in the carbonylation process and where are they located in the structure of mordenite. Furthermore, one should also find how H_2O interacts with the active sites and with the surface reaction intermediates. Such knowledge would certainly give leads for preparing an optimized zeolite catalyst in which the acid sites in specific positions of the zeolite have been generated.

We have investigated by means of quantum-chemical methods the stability and reactivity of methoxy groups at different T positions of mordenite in order to determine whether different positions within the 12- and 8MR channels show different reactivities and steric constraints to either the carbonylation reaction or the competing and undesired processes.[19,20] The reactions that we have considered here are the following:

(a) Formation of the methoxy groups from methanol:

$$Z{-}H + CH_3OH \rightarrow Z{-}CH_3 + H_2O \quad (1)$$

(b) Attack on the methoxy groups by CO, water, methanol, and DME:

$$Z{-}CH_3 + CO \rightarrow Z^- + CH_3CO^+ \quad (2)$$

$$Z{-}CH_3 + H_2O \rightarrow Z^- + CH_3OH_2^+ \quad (3)$$

$$Z{-}CH_3 + CH_3OH \rightarrow Z^- + (CH_3)_2OH^+ \quad (4)$$

$$Z{-}CH_3 + DME \rightarrow Z^- + (CH_3)_3O^+ \quad (5)$$

To completely clarify the role of water in the activity of mordenite for the carbonylation reaction, we have studied the competitive adsorption of water and methanol on Brønsted sites and the adsorption of water close to the methoxy groups. Finally, the complete reaction path for methanol carbonylation at one specific T position has been calculated. We propose here that only when the methoxy groups are formed in T3-O33 positions it is possible to achieve high carbonylation selectivities. It is shown that only in this situation, as a result of the unusual orientation of the methoxy group, the transition state for the attack of CO fits perfectly in the 8MR channel, while the undesired reactions leading to hydrocarbons cannot occur. From these results, the effect of water on the reaction rate is also explained on a molecular basis, and a global microkinetic model is proposed.

2. Theoretical Basis

Mordenite crystallizes in an orthorhombic *Cmcm* space group with lattice parameters $a = 18.094$ Å, $b = 20.516$ Å, and $c = 7.524$ Å and 144 atoms in the conventional unit cell.[21] Lattice projections along the *c* and *b* axes along with the atom-labeling scheme are shown in Figure 1. The silicon framework of mordenite is composed of four- and five-membered rings that link to form large 12MR channels parallel to *c* interconnected via 8MR side pockets parallel to *b*. There are four nonequivalent tetrahedral sites in the mordenite unit cell: T1 in the 12MR main channel, T2 and T4 in the intersection between the 12MR channel and the 8MR pocket, and T3 inside the 8MR pocket.

Four cluster models were cut out from the periodic structure of pure silica mordenite, each built around one different T position and containing the T position considered, the four $-OSi(OSi-)_3$ groups linked to it, and at least one 8MR or one 12MR. The dangling bonds that connect the cluster to the rest of the solid were saturated with H atoms 1.49 Å from the Si atoms and directed toward the positions occupied in the crystal by the oxygen atoms in the next coordination sphere. The sizes of the clusters modeling

(9) Cheung, P.; Bhan, A.; Sunley, G. J.; Iglesia, E. *Angew. Chem., Int. Ed.* **2006**, *45*, 1617.
(10) Cheung, P.; Bhan, A.; Sunley, G. J.; Law, D. J.; Iglesia, E. *J. Catal.* **2007**, *245*, 110.
(11) Jiang, Y.; Hunger, M.; Wang, W. *J. Am. Chem. Soc.* **2006**, *128*, 11679.
(12) Bhan, A.; Allian, A. D.; Sunley, G. J.; Law, D. J.; Iglesia, E. *J. Am. Chem. Soc.* **2007**, *129*, 4919.
(13) Blasco, T.; Boronat, M.; Concepción, P.; Corma, A.; Law, D.; Vidal-Moya, J. A. *Angew. Chem., Int. Ed.* **2007**, *46*, 3938.
(14) Esteves, P. M.; Louis, B. *J. Phys. Chem. B* **2006**, *110*, 16793.
(15) Zicovich-Wilson, C. M.; Corma, A.; Viruela, P. *J. Phys. Chem.* **1994**, *98*, 10863.
(16) Walspurger, S.; Sun, Y.; Sido, A. S. S.; Sommer, J. *J. Phys. Chem. B* **2006**, *110*, 18368.
(17) Nesterenko, N. S.; Thibault-Starzyk, F.; Montouillout, V.; Yuschenko, V. V.; Fernández, C.; Gilson, J. P.; Fajula, F.; Ivanova, I. I. *Microporous Mesoporous Mater.* **2004**, *71*, 15.
(18) Boronat, M.; Viruela, P. M.; Corma, A. *J. Am. Chem. Soc.* **2004**, *126*, 3300.
(19) Lesthaeghe, D.; Van Speybroeck, V.; Marin, G. B.; Waroquier, M. *Angew. Chem., Int. Ed.* **2006**, *45*, 1714.
(20) Lesthaeghe, D.; Van Speybroeck, V.; Marin, G. B.; Waroquier, M. *Ind. Eng. Chem. Res.* **2007**, *46*, 8832.
(21) Alberti, A.; Davoli, P.; Vezzalini, G. *Z. Krystallogr.* **1986**, *175*, 249.

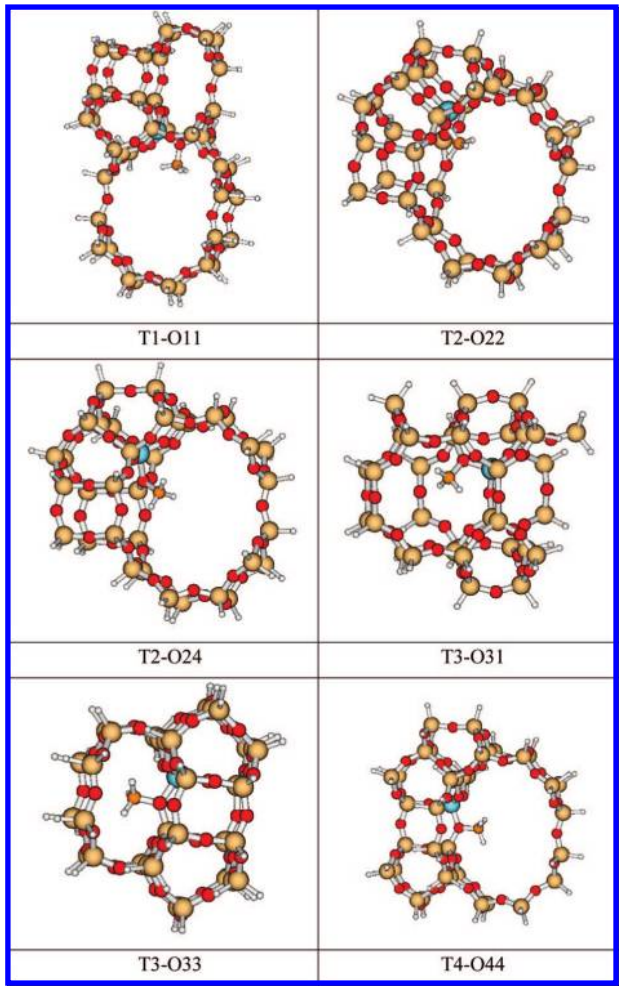

Figure 2. Cluster models used in this work, each showing the orientation of the methoxy group.

Table 1. Orientations of the Methyl Groups Formed on the Different O Atoms in MOR

points to:	O11	O22	O33	O44	O12	O31	O24	O34	%
12MR	8			4	16				29
8MR mouth		8					16		25
8MR bottom	8		4			16			29
5MR		8						8	17

Table 2. Calculated Reaction Energies (kcal/mol) for the Process $Z{-}H + CH_3OH \rightarrow Z{-}CH_3 + H_2O$ and Optimized Values of the C−O distance (Å) in the Methoxy Group

	ΔE	$r(O_{MOR}{-}C)$
T1-O11	4.1	1.481
T2-O22	7.1	1.494
T2-O24	2.5	1.478
T4-O44	0.2	1.476
T3-O33	1.3	1.464
T3-O31	8.4	1.481

T1, T2, T3, and T4 were 148, 125, 121, and 130 atoms, respectively. An Al atom was then introduced into the selected T position, and a methoxy group was formed on each of the four different O atoms bonded to Al. Table 1 shows the orientations of the methoxy groups formed on the different O atoms in MOR, following the labeling shown in Figure 1. From among all of these positions, we selected those depicted in Figure 2: Al in T1 and the methoxy group on O11 (T1-O11), Al in T2 and the methoxy group on either O22 (T2-O22) or O24 (T2-O24), Al in T3 and the methoxy group on either O31 (T3-O31) or O33 (T3-O33), and finally, Al in T4 and the methoxy group on O44 (T4-O44). It can be seen that only the T3-O31 and T3-O33 positions are located inside the 8MR pockets and are therefore inaccessible to probe molecules such as pyridine. The rest of the positions considered above either point to the 12MR channels or are located at the pore mouth. With the use of these clusters to simulate the solid catalyst, the geometries of all of the species considered in this work (both minima and transition states) were optimized by means of the ONIOM scheme[22] as implemented in the Gaussian 03 computer program.[23] The ONIOM approach subdivides the *real* system into a *model* system, which is described at the highest level of theory, and several other parts or layers, computed at progressively lower and computationally cheaper levels of theory. In the present work, the model system included the Al atom, the four O atoms in the first coordination sphere, the four Si atoms bonded to them, the proton of the Brønsted acid site, and the organic molecules studied. The coordinates of these atoms were completely optimized using density functional theory (DFT) with the B3PW91 functional,[24] the standard 6-311G(d,p) basis set for C, O, and H, and the 6-31G(d,p) basis set for Si and Al.[25] The rest of the system was treated at the semiempirical MNDO level,[26] and no geometry optimization was performed for these atoms. Finally, single-point calculations in which all of the atoms were treated at the highest DFT level were performed.

Table 3. Optimized Values of the Most Important Distances (Å) in the Transition States for the Attack of CO, H_2O, CH_3OH, and DME on Different Methoxy Groups in MOR

	CO		H_2O		CH_3OH		DME	
	$r(O_Z{-}C)$	$r(C{-}C_{CO})$	$r(O_Z{-}C)$	$r(C{-}O)$	$r(O_Z{-}C)$	$r(C{-}O)$	$r(O_Z{-}C)$	$r(C{-}O)$
T1-O11	2.029	1.973	2.155	1.853	2.064	1.917	2.032	1.920
T2-O22	2.043	2.022	2.111	1.934	2.034	1.980	2.003	2.001
T2-O24	2.014	1.973	2.110	1.864	2.029	1.917	2.000	1.938
T4-O44	2.018	1.935	2.151	1.822	2.062	1.862	2.024	1.872
T3-O33	1.976	1.908	2.246	1.655	2.198	1.747	2.899	2.087
T3-O31	1.964	1.907	2.153	1.788	2.037	1.854	1.972	1.859

3. Results and Discussion

3.1. Stability of Methoxy Groups. The initial methanol adsorption in acid zeolites and its decomposition into water and a methoxy group has been widely investigated as a possible pathway for dehydration of methanol to dimethyl ether (DME). It is accepted that methanol is chemisorbed as a methoxonium cation $CH_3OH_2^+$ that in a second step decomposes into water and a methoxy group, with the activation barrier of the process being lower in the presence of other water or methanol molecules.[19] In this work, however, we intended to compare the abilities of different positions in mordenite to form surface methoxys from methanol, and therefore, we only considered the stability of the products, namely, the surface methoxy plus water, relative to the reactants, which are the Brønsted acid site plus methanol. The calculated reaction energies and lengths of the C−O bond in the methoxy group are summarized in Table 2. It can be seen that formation of a methoxy group is endothermic in all cases, with the T3-O31 and T2-O22 positions

(22) (a) Svensson, M.; Humbel, S.; Froese, R. D. J.; Matsubara, T.; Sieber, S.; Morokuma, K. *J. Phys. Chem.* **1996**, *100*, 19357. (b) Humbel, S.; Sieber, S.; Morokuma, K. *J. Chem. Phys.* **1996**, *105*, 1959.
(23) Frisch, M. J.; et al. *Gaussian 03*, revision B.04; Gaussian, Inc.: Pittsburgh, PA, 2003.
(24) (a) Becke, A. D. *J. Chem. Phys.* **1993**, *98*, 5648. (b) Perdew, J. P.; Wang, Y. *Phys. Rev. B* **1992**, *45*, 13244.
(25) Hariharan, P. C.; Pople, J. A. *Theor. Chim. Acta* **1973**, *28*, 213.
(26) (a) Dewar, M. J. S.; Thiel, W. *J. Am. Chem. Soc.* **1977**, *99*, 4907. (b) Davis, L. P.; Guidry, R. M.; Williams, J. R.; Dewar, M. J. S.; Rzepa, H. S. *J. Comput. Chem.* **1981**, *2*, 433.

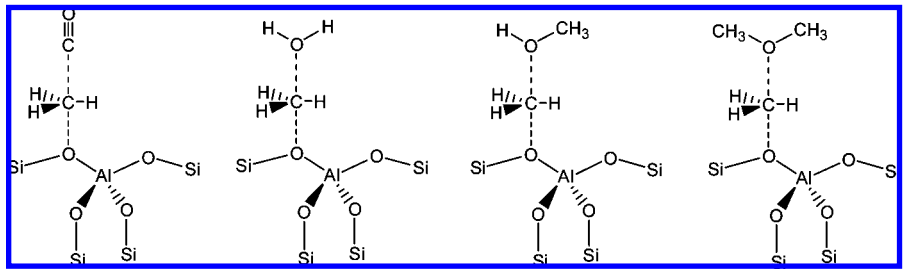

Figure 3. Transition states for the attack of (a) CO, (b) H_2O, (c) CH_3OH, and (d) DME on a surface methoxy group.

Table 4. Calculated Activation Energies (kcal/mol) for the Attack of CO, H_2O, CH_3OH, and DME on Different Methoxy Groups in MOR

	CO	H_2O	CH_3OH	DME
T1-O11	23.9	12.7	9.9	10.4
T2-O22	20.0	8.5	7.0	6.7
T2-O24	23.3	11.8	8.8	9.1
T4-O44	25.6	13.8	11.8	11.0
T3-O33	23.5	11.3	19.9	55.7
T3-O31	28.1	14.0	15.0	26.3

being significantly unfavorable from a thermodynamic point of view. The most stable methoxys are formed on T3-O33 sites, which are located inside the 8MR pockets, and on T4-O44 and T2-O24 at the pocket mouth, pointing to the 12MR channels. The stability of the formed methoxy group seems to be somehow related to the length of the C−O bond, although there is not a linear correlation.

3.2. Interaction of Methoxy Groups with CO, H_2O, CH_3OH, and DME. The reaction of a methoxy group with a nucleophilic reactant such as CO, H_2O, CH_3OH, or DME involves in all cases the transfer of a cationic CH_3^+ fragment to the nucleophile molecule from the framework oxygen O(Z) to which it was covalently bonded (see Figure 3). The geometry of the transition state is linear, with the four atoms of the CH_3^+ fragment lying in a plane perpendicular to the line linking the framework oxygen O(Z) and either the carbon atom of CO or the oxygen atom of H_2O, CH_3OH, or DME. The calculated values for the O(Z)−C(CH_3^+)−C(CO) and O(Z)−C(CH_3^+)−O(H_2O, CH_3OH, DME) angles are close to 180° in most cases. The cationic CH_3^+ fragment is in general slightly closer to the attacking molecule than to the framework oxygen, with the difference between the two distances being most noticeable in the case of H_2O (Table 3). The reaction product is in most cases a cationic species that is stabilized by the zeolite framework.

It should be mentioned that a possible mechanism for carbonylation in which CO is initially activated by interacting with a Brønsted acid site or a Lewis acid center before reacting with the methoxy group has been suggested.[10,13] However, the interaction of CO with Brønsted acid sites is very weak (see below), and all of our attempts to find a complex with CO attached to the framework Al and being inserted laterally into the O(Z)−O(CH_3^+) bond failed, with the restricted species obtained being considerably less stable than those discussed here.

Calculated activation energies for the reaction Z−CH_3 + X → Z^- + (X−CH_3)$^+$, where X is CO, H_2O, CH_3OH, or DME, are summarized in Table 4. The first remarkable result is that CO attack always involves the highest activation barrier, this being between 20 and 28 kcal/mol depending on the position occupied by the methoxy group. The activation barriers for the attack of H_2O, CH_3OH, and DME are 11−14 kcal/mol lower when the methoxy group is accessible from the 12MR main channels. When the methoxy group is inside the 8MR pockets, as for the T3-O33 and T3-O31 positions, the activation energies for the attack of H_2O are comparable to those obtained for the other positions, but the activation barriers for the attack of CH_3OH and DME are considerably higher. The reason for this is related to the geometry of the transition state and can be clearly observed in Figure 4. In the transition state, the angle formed by the framework oxygen O(Z), the carbon of the transferring CH_3^+ group, and either the C of CO or the O of the other three attacking molecules is close to 180°, and the CH_3^+ fragment is approximately halfway between the two other

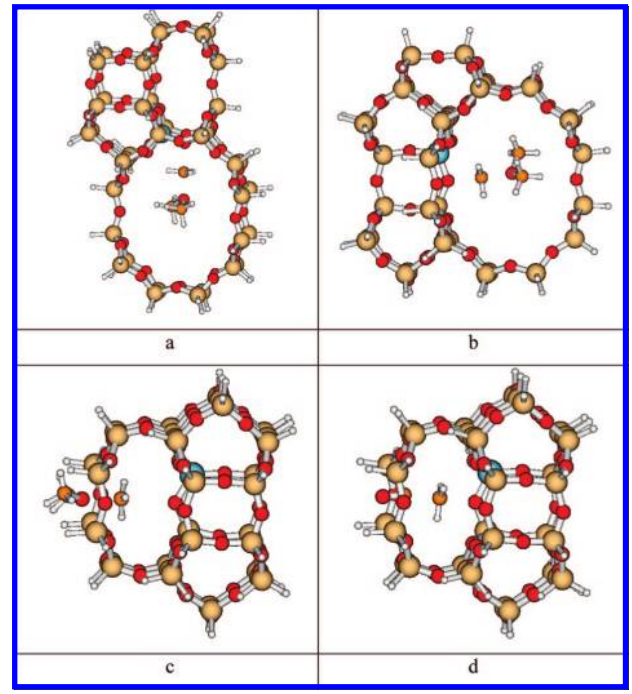

Figure 4. Optimized geometries of the transition states for the reaction of DME with a methoxy group at (a) T1-O11, (b) T4-O44, and (c) T3-O33 and for (d) the reaction of CO with a methoxy group at T3-O33.

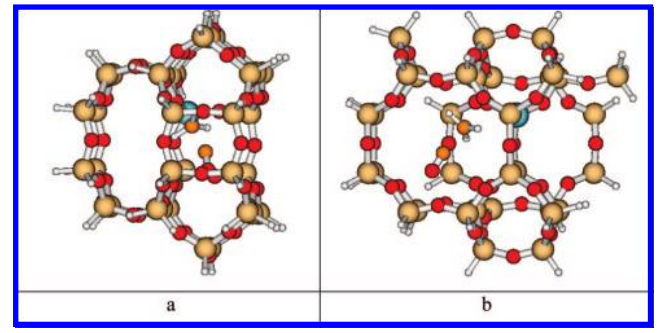

Figure 5. Optimized geometry of the transition state for the reaction of a methoxy group at T3-O31 with CO: (a) side view; (b) front view.

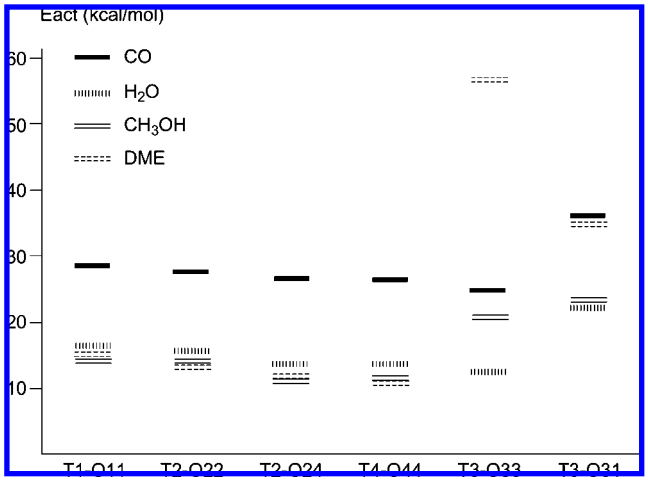

Figure 6. Calculated apparent activation energies (kcal/mol) for the reactions of CO, H_2O, CH_3OH, and DME with methoxy groups at different positions of MOR.

atoms. When the methoxy group is pointing to the 12MR main channel (T1-O11 and T4-O44) or at the pocket mouth (T2-O22 and T2-O24), the attacking molecule comes from the large channel, and the transition state is formed in such a way that it preferentially occupies the space in the 12MR channel. When the methoxy group is at the T3-O33 position, it is accessible to attacking molecules that come from the large channel through an 8MR double ring. Both CO and H_2O can easily diffuse through this channel; however, CH_3OH is somewhat hindered, and it is completely impossible for DME to get inside the pocket with the O atom pointing to the methoxy group. As a result, the optimized $O(Z)-C(CH_3^+)$ distance in the transition state is almost 3 Å while the $C(CH_3^+)-O(DME)$ distance cannot be shorter than 2 Å (Table 3), and the structure is therefore highly unstable.

The situation in the case of T3-O31 is slightly different, as shown in Figure 5. The methoxy group is initially in the plane of the 8MR ring and by interaction with the attacking molecules moves from this plane and orientates toward the 8MR double ring through which these molecules arrive, in such a way that it becomes difficult to maintain the linearity of the $O(Z)-C(CH_3^+)-C(CO)$ and $O(Z)-C(CH_3^+)-O(H_2O, CH_3OH,$ DME) angles. Thus, the calculated values for these angles in T3-O31 are ~170°, while they are close to 180° in all of the other positions. This is reflected in slightly higher activation energies in relation to those obtained at the positions accessible from the 12MR main channel.

3.3. Reaction Selectivity at the Different T Positions. In order to clearly determine whether one or more T positions are selective for a given reaction, we should consider the whole process from the beginning, that is, not only the activation energy for the reaction of the methoxy group but also the energy necessary to form this methoxy group. The activation energies relative to the initial reactants, the Brønsted acid site plus methanol, are plotted in Figure 6. This graph clearly shows that the carbonylation reaction is kinetically disfavored at all positions accessible from the main 12MR channel. In these cases, dehydration of methanol to DME and subsequent formation of hydrocarbons competes with the methanol carbonylation, and the selectivity for producing acetic acid and/or acetate is low. However, for the Al atom at T3, inside an 8MR pocket, the situation is completely different. If the methoxy group is formed on T3-O31, the activation energies for the first steps of

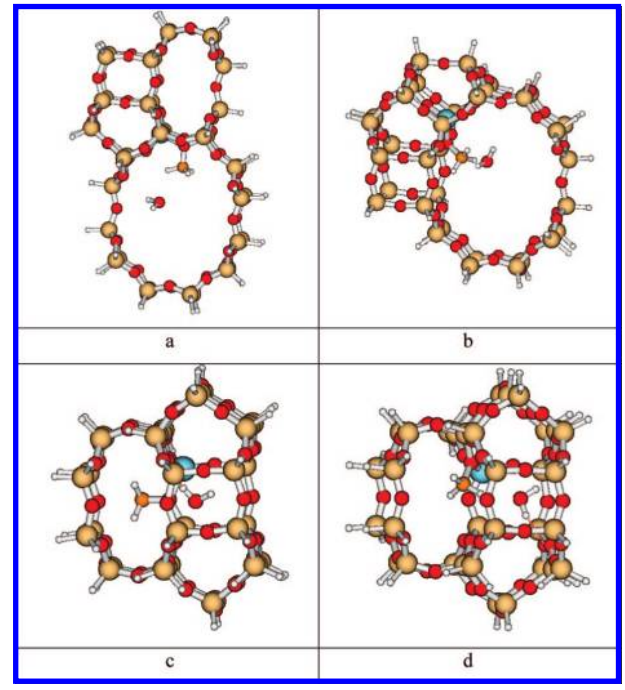

Figure 7. Optimized geometries of H_2O adsorbed near a methoxy group in (a) T1-O11, (b) T2-O24, (c) T3-O33, and (d) T3-O31.

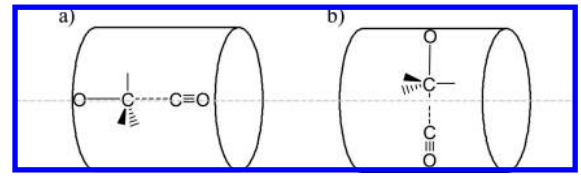

Figure 8. Schematic representation of the relative orientation of the $O_{framework}-CH_3$ bond and the channel axis at (a) the T3-O33 position of MOR and (b) any other position in an 8MR channel.

the carbonylation and hydrocarbon-formation reaction mechanisms are comparable. However, as discussed in section 3.1, for Al at T3, the methoxy group is more likely to be formed on T3-O33. In this case, and for the reasons discussed above, the transition state for the attack of DME on the methoxy group is highly destabilized, and therefore, the activation barrier for the carbonylation reaction is considerably lower than that for hydrocarbon formation. Moreover, the activation barrier for the attack of methanol to form DME is not too different from that obtained for carbonylation. Altogether, it is found that the selectivity toward methanol carbonylation is highest for the Al at T3 and, more specifically, when the methoxy group is at T3-O33, this being the only position that is clearly selective.

3.4. Negative Effect of Water on the Carbonylation Rates. It is also clear from Figure 6 that the reaction of H_2O with the methoxy groups to give methanol is kinetically favored at all positions. This result, together with the fact that formation of methoxy groups from methanol is slightly endothermic at all positions (Table 2) may explain on one hand the induction period observed by Cheung et al.,[10] which reflects the slow replacement of protons by methoxy groups, and on the other hand the negative effect of water on the carbonylation reaction rates.[9] Since the reaction of methanol with a Brønsted acid site to give a methoxy group and water is an equilibrium, addition of water displaces the equilibrium toward the reactants, decreasing the number of methoxy groups available for reaction with CO.

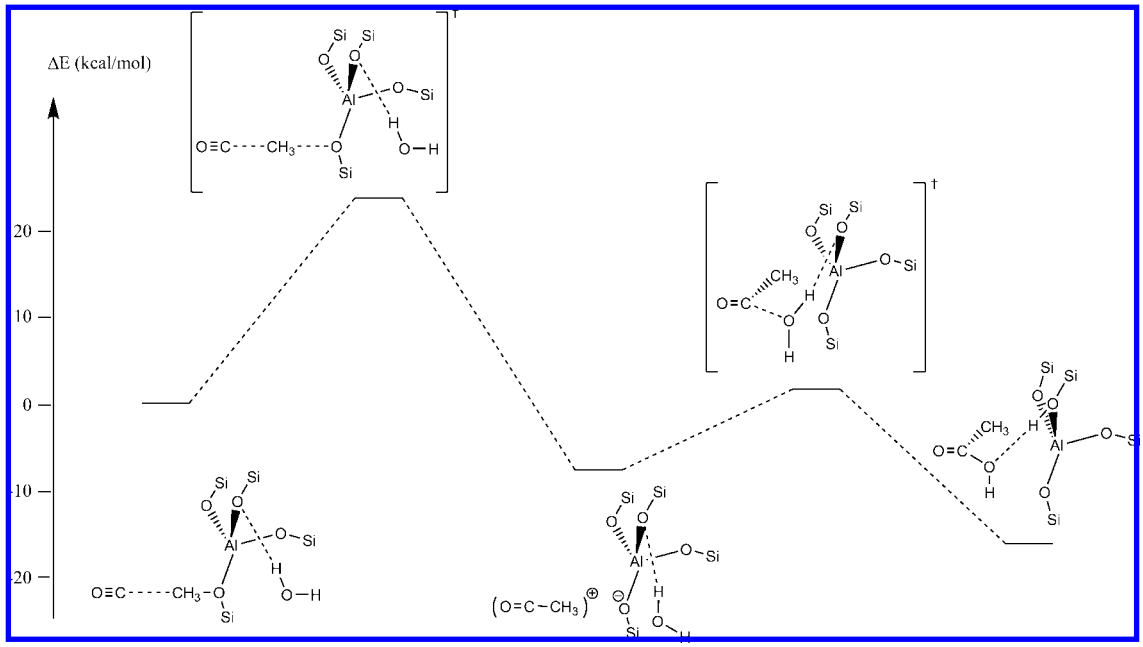

Figure 9. Calculated energy profile for methanol carbonylation at the T3-O33 position.

Table 5. Calculated Energies (kcal/mol) for the Adsorption of CO, H_2O, and CH_3OH on Different Brønsted Acid Sites in MOR and for the Adsorption of H_2O near a Methoxy Group

	CO (Z−H)	H_2O (Z−H)	CH_3OH (Z−H)	H_2O (Z−CH_3)
T1-O11	−5.7	−21.2	−21.8	−6.7
T2-O22	−5.8	−23.2	−22.5	−3.7
T2-O24	−5.5	−23.0	−20.7	−11.2
T4-O44	−6.4	−23.5	−26.3	−6.1
T3-O33	−3.6	−24.1	−14.6	−9.5
T3-O31	−2.7	−18.6	−14.4	−10.5

Other reasons have been proposed[9,10] to explain the inhibition of the carbonylation reaction rates when water is added, such as competitive adsorption of water and methanol on Brønsted acid sites or adsorption of water near the methoxy groups, making them inaccessible to CO without decomposing them. The calculated energies for adsorption of CO, H_2O, and CH_3OH on different Brønsted acid sites in MOR and of H_2O close to the methoxy groups are listed in Table 5. The interaction of CO with Brønsted acid sites is weak, suggesting that this molecule is not initially activated and reacts directly with methoxy groups. Adsorption of H_2O and CH_3OH on the Brønsted acid sites accessible from the 12MR main channel is competitive, and this may have an influence on the induction period at the beginning of the reaction. The situation is still worse inside the 8MR pockets. Adsorption of water is clearly more favorable than that of methanol, and therefore, the initial formation of methoxy groups in T3-O33 and T3-O31 is slower.

The reaction of methanol with a Brønsted acid site results in the formation of a surface methoxy group and a H_2O molecule that will probably remain in the vicinity of the methoxy group and either form a hydrogen bond with one of the basic oxygens directly bonded to Al, coordinate to the Al atom, which may act as a Lewis acid center, or just weakly interact with the methoxy group. All of these possibilities were extensively investigated here, and in no case was a direct interaction between H_2O and the Al atom found. At the four positions where the methoxy group points to the 12MR channel, the H_2O formed does not interact with a neighboring basic oxygen but instead occupies the space in the large channel and is located ∼3 Å from the carbon atom of the methoxy group, with the water oxygen atom weakly interacting with one of the hydrogens of the methoxy group (see Figure 7a,b). It is possible that this molecular disposition hinders the attack of CO to give the carbonylation reaction. However, when the methoxy group is inside the 8MR pockets, this type of complex is not formed. When the methoxy group is at the T3-O33 position, H_2O either diffuses through the 8MR channel to the 12MR channel or binds to one of the framework oxygen atoms that is bonded to Al but points to the 8MR channel behind the methoxy group, as depicted in Figure 7c. Finally, when the methoxy group is on T3-O31, the oxygen atom of H_2O interacts with one of the hydrogens of the methyl group, but as shown in Figure 7d, the molecule is placed not in front of the methoxy group but at one side in the 8MR channel. The adsorption energies obtained for H_2O inside the 8MR pockets are similar to those obtained for the other T positions, but this molecular arrangement leaves the methoxy group completely free to react with CO. It should be remarked that it was not possible to obtain water adsorption complexes of this type at the other T positions, and geometry optimizations led in all cases to the complexes previously described and shown in Figure 7a,b.

It can thus be concluded that the negative effect of water on the carbonylation reaction rates is mainly related to the competitive adsorption of water and methanol on the Brønsted acid sites and to the displacement of the methanol ⇄ methoxy equilibrium toward the reactants when water is added. Adsorption of water near the already formed methoxy groups does not seem to have a remarkable influence on the reaction rates.

3.5. Special Features of the T3-O33 Position. Up to now it has been found that methanol carbonylation occurs selectively only for Al at the T3 position with the methoxy group attached to O33. However, as we have seen above, the catalytic behavior of this special position is related not only to the size of the channel in which it is located but also to the unusual orientation of the methoxy group in relation to the channel. As shown in Figure 8, if we consider the 8MR channel to be a cylinder, the bond between the methoxy group and the framework oxygen at the T3-O33 position in mordenite is parallel to the cylinder axis, while in all other

positions, as well as in other zeolites containing 8MR channels, this bond is more or less normal to the cylinder axis. As we have seen, the attack of CO and other nucleophiles occurs through a linear transition state that follows the orientation of the O(Z)−CH_3 bond. When the methoxy group is at the T3-O33 position, the transition state for the attack of a small linear molecule such as CO fits perfectly in the 8MR channel, while the reaction with bulkier nucleophiles is sterically impeded. However, when the methoxy group is either at the T3-O31 position of MOR or in an 8MR channel of any other zeolite, with the O(Z)−CH_3 bond not parallel to the channel axis, such a linear transition state will be sterically destabilized regardless of the size of the attacking nucleophile. This would explain the much lower activity and selectivity of ferrierite in comparison with mordenite, although both zeolites contain 8MR rings.

3.6. Complete Reaction Path for Methanol Carbonylation. Finally, the complete reaction path for the carbonylation of methanol at the T3-O33 position was calculated. To do this, it was assumed that the first step, namely, formation of the surface methoxy from adsorbed methanol, had already occurred, and the structure depicted in Figure 7c, with water interacting with the neighboring basic oxygen, was used to model this initially formed methoxy group. The interaction of CO with the methoxy group is negligible, and therefore, the origin for the energies in the calculated profile depicted in Figure 9 is the sum of the energies of CO and the complex depicted in Figure 7c. As discussed in section 3.2, the attack of CO on the methoxy group involves the transfer of a cationic CH_3 fragment from the framework oxygen O(Z) to CO. The O(Z)−C(CH_3^+) and C(CH_3^+)−C(CO) distances in the transition state are 1.98 and 1.94 Å, respectively, and the O atom of the coadsorbed H_2O molecule is 2.01 Å from one of the H atoms of the transferring methyl cation (see Figure 10a). Since H_2O is not directly involved in any bond-breaking or bond-forming process, it does not help to stabilize the transition state, and the calculated activation energy is 23.9 kcal/mol, which is equivalent to that reported in Table 4 for the model without coadsorbed water. An acylium cation that is 6.9 kcal/mol more stable than the initial reactants is formed in this step (see Figure 10b). This structure, which was characterized as a true reaction intermediate, is stabilized by the zeolite framework through local hydrogen interactions between the methyl group and the nearest oxygen atoms and by medium- and long-range electrostatic effects. The coadsorbed H_2O molecule also now strongly interacts with the acylium cation, as reflected in the calculated H(CH_3^+)−O(H_2O) distance, which has decreased to 1.55 Å. Moreover, as the system evolves to a more ionic situation, the oxygen atoms bonded to Al become more negatively charged and the hydrogen bond with the coadsorbed H_2O becomes stronger. This is reflected in a shortening of the H(H_2O)−O(Z) distance from 1.86 Å in the initial complex to 1.75 Å in the transition state to 1.59 Å in the reaction intermediate. In a second step, through the transition state depicted in Figure 10c, H_2O reacts with the acylium cation to form acetic acid. The process involves decomposition of H_2O into a OH group that bonds to the central C atom of the acylium cation, forming acetic acid, and a proton that is transferred to a framework O, restoring the zeolite Brønsted acid site. The calculated activation barrier for this step is low, only 7.5 kcal/mol, in agreement with experimental results indicating that the rate-determining step is the reaction of CO with the surface methoxy groups,[10,13] and the reaction product is 9.8 kcal/mol more stable than the reaction intermediate.

It is important to remark that the catalytic cycle described above ends with acetic acid adsorbed on a Brønsted acid site, so the second catalytic cycle should start with methoxy formation from adsorbed methanol. However, the acylium cation intermediate could also react with CH_3OH or DME instead of H_2O. The process would involve formation of a bond between the O atom of CH_3OH or DME and the central C atom of the acylium cation and the transfer of either a proton (from CH_3OH) or a cationic CH_3^+ fragment (from CH_3OH or DME) to the framework O31 atom. In the latter case, the methoxy group would be formed at the same time as the acetic acid or methyl acetate product, and therefore, the initial step of methoxy formation from adsorbed methanol would be avoided. The transition state for the reaction of the acylium cation intermediate with CH_3OH to yield methyl acetate and a Brønsted acid site

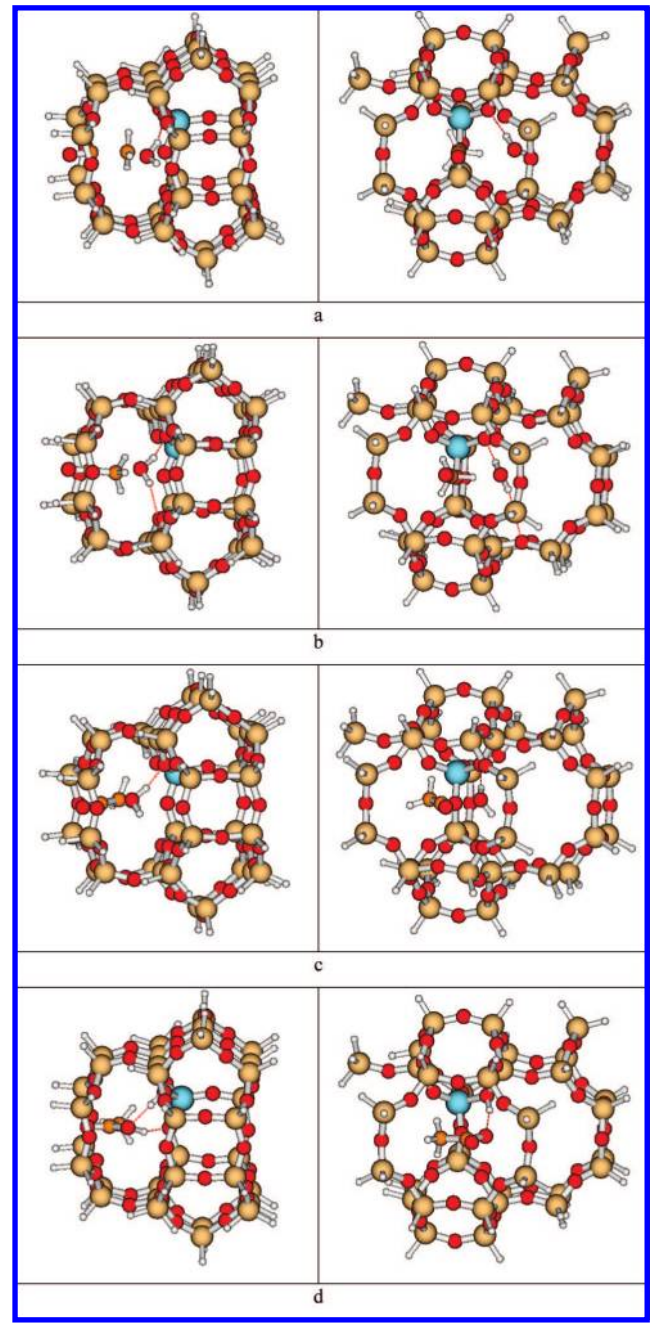

Figure 10. (left) Side views and (right) face views of the optimized structures involved in the mechanism of methanol carbonylation at the T3-O33 position in MOR: (a) transition state for the attack of CO on the methoxy group; (b) acylium cation reaction intermediate; (c) transition state for the reaction of water with the acylium cation reaction intermediate; and (d) acetic acid adsorbed on the restored Brønsted acid site.

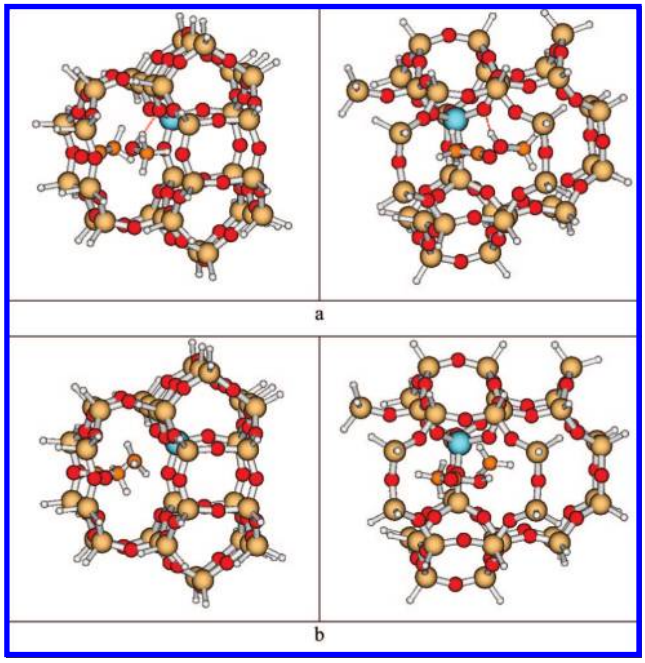

Figure 11. (left) Side views and (right) face views of the optimized structures of the two different transition states obtained for the reaction of methanol with the acylium cation intermediate formed at the T3-O33 position in MOR: (a) reaction products are methyl acetate and a Brønsted acid site; (b) reaction products are acetic acid and a methoxy group.

(Figure 11a) is similar to that obtained for the reaction of the acylium cation with water (Figure 10c), as is the calculated activation energy for the process, 7.2 kcal/mol. However, the reaction of the acylium cation intermediate with CH_3OH to give acetic acid and a surface methoxy group is considerably more difficult. In this case, the transfer of the CH_3^+ group between the two oxygen atoms occurs through a linear transition state (Figure 11b) in which the methyl carbon is 2.108 Å from O31 and 1.878 Å from the O atom of CH_3OH. This structure is quite unstable in such a restricted space, and the calculated activation energy rises to 34.5 kcal/mol. A similarly high activation energy can also be expected for the reaction of DME with the acylium cation intermediate, since the process necessarily involves the transfer of a methyl cation with the subsequent formation of a surface methoxy group. However, it has been shown experimentally that the reaction occurs with DME at a higher reaction rate.[10,12] This observation implies that when DME reacts with the acylium cation intermediate to give methyl acetate, the new methoxy group is not formed at the same site where the acylium cation was adsorbed but at a different Al site. Thus, on the bases of our calculations and the reported experimental results,[10,12] we propose that the activation of DME occurs at a second T3 center also located in the 8MR channel, as shown in Figure S1 in the Supporting Information. We believe that the presence of Al pairs inside the 8MR channel is not only convenient for stabilizing charged species[10] but also mandatory for the formation of methyl acetate as a primary product and the simultaneous regeneration of the methoxy group in the reaction with DME. We are now theoretically investigating this reaction path using larger clusters as models for Al pairs inside the 8MR channel.

4. Conclusions

The mechanism of methanol carbonylation at different positions of zeolite MOR has been investigated theoretically in order to discover which are the active sites that can selectively catalyze the desired reaction and therefore how the existing catalysts can be improved. The following conclusions have been obtained:

1. The most stable methoxys are formed on T4-O44 positions pointing to the 12MR channel and on T3-O33 positions located inside the 8MR pockets. On the other hand, the methoxy groups formed on T3-O31, which are also located inside the 8MR pockets, are among the less stable.
2. When the methoxy groups are located at any position pointing to the 12MR channel (i.e., Al at T1, T2, or T4), formation of DME and hydrocarbons is kinetically favored over carbonylation.
3. The T3-O33 position is the only one that is clearly selective for carbonylation. When the methoxy group is at the T3-O33 position inside the 8MR channel, the transition state for the attack of DME is highly destabilized and the activation barrier for carbonylation is considerably lower than that for hydrocarbon formation. On the other hand, the activation energy for attack of methanol to form DME is comparable to that for carbonylation.
4. The special catalytic behavior of the T3-O33 position is related not only to the size of the channel in which it is located but also to the unusual orientation of the methoxy group in relation to the channel (parallel to the cylinder axis). The transition state for the attack of CO fits perfectly well in the 8MR channel, while the reactions with bulkier nucleophiles are sterically impeded.
5. The experimentally observed negative effect of water on the carbonylation reaction rates is related on one hand to the competitive adsorption of water and methanol on the Brønsted acid sites and on the other hand to the displacement of the equilibrium $Z{-}H + CH_3OH \rightleftarrows Z{-}CH_3 + H_2O$ toward the reactants, which decreases the number of methoxy groups available for reaction with CO. This could be avoided, at least in part, by adding a species that preferentially adsorbs water without interfering in the reaction mechanism.
6. The rate-determining step in the mechanism of methanol carbonylation is attack on the methoxy group by CO to form an acylium cation intermediate that is stabilized by the zeolite framework. Reaction of H_2O with the acylium cation produces acetic acid and a Brønsted acid site, while reaction of CH_3OH with the acylium cation preferentially produces methyl acetate and a Brønsted acid site.
7. Reaction of DME with the acylium cation intermediate produces methyl acetate and a methoxy group. Although the activation energy for this step is higher than that for the reaction with H_2O, a methoxy group is formed at the same time, and therefore, the initial step of methoxy formation from methanol would be avoided. This could explain the higher reaction rates obtained when DME instead of methanol is used as a feed.

Acknowledgment. The authors thank BP Chemicals for financial support and permission to publish these results and also thank CICYT (Project MAT2006-14274-C02-01) for financial support.

Supporting Information Available: Figure S1 and complete ref 23. This material is available free of charge via the Internet at http://pubs.acs.org.

JA805607M